Bioorthogonal tools to study fatty acid uptake in immune cells

Bertheussen, K.

5

Summary & Future Prospects

Summary

The cellular metabolism of immune cells constitutes an important part of their proper function and activation.[1] Using T cells as an example, this phenomenon is highlighted by the metabolic reprogramming that occurs in these cells upon activation. The metabolism of quiescent T cells mainly revolves around catabolic pathways where glucose (for naïve T cells) or fatty acids (for memory T cells) are broken down to feed the tricarboxylic acid (TCA) cycle and oxidative phosphorylation (OXPHOS) pathways to generate energy via mitochondrial respiration.[2] Upon activation and differentiation, effector T cells shift their metabolism from mitochondrial respiration to aerobic glycolysis. Glycolysis is an important pathway to generate building blocks for the synthesis of complex biomolecules, so the metabolic reprogramming is accompanied by a shift towards anabolic pathways, generating the necessary biomaterials for increased growth and proliferation.[3] The metabolic reprogramming is further supported by an increased uptake of exogenous nutrients, such as glucose, amino acids, and fatty acids (FAs). The availability of these nutrients in the cell's environment is essential for the proper activation and differentiation of effector T cells.[4–8] The ability to unravel this complex interface between the immune system and cellular metabolism relies on the development of appropriate chemical tools. The aim of this thesis was to develop sterculic acid (StA) as a bioorthogonal analogue of the immunomodulatory FA oleic acid (OA), and to use this as a tool to study the uptake of StA in different immune cells.

Chapter 1 gave a detailed description of the current understanding of T cell metabolism and how it is connected to their immunological functions. A special focus was given to FA and lipid metabolism, explaining how pathways like fatty acid β-oxidation (FAO), fatty acid synthesis (FAS), and FA uptake are regulated in different T cell subsets. Furthermore, a deep dive into the function of the monounsaturated OA (C18:1, ω-9) as an immunomodulatory FA was given, where OA has been shown to influence immunological functions in diseases like asthma, sepsis, and cancer. Specifically for T cells, OA has been shown to affect their proliferation, metabolism and differentiation. Chapter 1 continues by describing molecular tools that are available for studying cellular uptake of exogenous FAs. Historically, either radioactively or fluorescently labelled FAs have been used for this purpose, but here it is suggested that bioorthogonal chemistry is more suitable for studying FA uptake. By incorporating a small chemical modification with a unique bioorthogonal functional group into the FA molecule, treating cells with this bioorthogonal FA analogue, and subsequently adding a reporter molecule (e.g. a fluorophore) with the complementary functionality, the FA analogue is covalently labelled in the cells. Chapter 1 proposed the naturally occurring plant metabolite StA as a novel live-cell compatible bioorthogonal analogue of OA and hypothesised that the cyclopropene moiety of StA would allow for an inverse electron-demand Diels-Alder (IEDDA) reaction with a tetrazine modified reporter molecule.

Chapter 2 described the initial exploration of StA as a bioorthogonal OA analogue. It focused on a library of eight quenched tetrazine-conjugated fluorophores and evaluated their abilities to react with StA via an IEDDA reaction. Their stability, as well as their turn-on ratio and reaction kinetics, were evaluated upon ligation with StA. These assays indicated that the IEDDA reaction between StA and the tetrazine-conjugated fluorophores could occur with varying efficiency in solution. Subsequently,

it was demonstrated by confocal microscopy that StA could be taken up by live cells, and the IEDDA reaction could be successfully performed on either live or fixed cells. Fluorophore **6,** a BODIPY FL-based conjugate with a H-substitution on the tetrazine, was deemed best for fixed-cell imaging, whereas fluorophore **7**, a BODIPY-based conjugate with a methyl-substitution on the tetrazine, was deemed best for live-cell imaging. The turn-on ratio of fluorophore **7** was sufficient to perform live-cell confocal imaging without washing away unreacted fluorophore, a big advantage to reduce cell loss during washing steps. Lastly, the labelling of StA *in cellulo* was multiplexed with two other bioorthogonal reactions to label several biomolecules simultaneously, emphasising the strength and flexibility of this novel bioorthogonal OA analogue.

Chapter 3 further delved into the diversity of StA as a bioorthogonal OA analogue by investigating its incorporation into proteins as a post-translational modification (PTM). Protein lipidation as a PTM is important for correct protein function, signalling, transportation and regulation, and can also have immunomodulatory properties. It was shown by fluorescent gel electrophoresis that StA could be incorporated into proteins as a PTM, and that the protein lipidation could be visualised by IEDDA reaction with tetrazine-conjugated fluorophores. However, the detected proteins depended on which fluorophore was used and whether the IEDDA reaction was performed on live cells or on cell lysate. To further investigate these observed differences in lipidation pattern, a pull-down chemical proteomics approach was applied. A library of cell-permeable tetrazine-modified biotin molecules were synthesised with different spacer lengths and substitutions on the tetrazine, and was compared to the commercially available, cell-impermeable biotin-PEG4-tetrazine. With fluorescent microscopy, it was demonstrated that biotins **17**, with a short spacer and methyl-substituted tetrazine, and **19**, with a longer spacer and H-substituted tetrazine, were cell-permeable and reactive with StA. Comparing the lipidated proteins that were recovered with **17**, **19**, or biotin-PEG4-tetrazine in a pull-down chemical proteomics approach showed little to no overlap between detected proteins. This further supported the previous observation that the timing of the IEDDA reaction makes a difference, but it also implied that chemical properties of the biotin molecules, such as spacer length, could also influence the pool of proteins that were detected. The developed method detected several proteins with known immunological functions, that have never been known to be lipidated as a PTM. Among them is SLC15A3, a transmembrane amino acid transporter with immunomodulatory properties. These results could indicate modification with OA as a novel regulatory mechanism for this protein.

In **Chapter 4**, the use of StA as a bioorthogonal OA analogue was applied to study the uptake of exogenous FAs in a heterogeneous, primary T cell population. After StA uptake and IEDDA reaction with fluorophore **7**, the cells were differentiated based on low or high uptake of StA by fluorescence-activated cell sorted (FACS). Comparing the low- and high-uptake populations with each other revealed remarkable phenotypic, metabolic, proteomic, and transcriptomic differences. The high-uptake cells took on a more effector-like phenotype with larger and more granulated cells, increased expression of CD44, and decreased expression of CD62L, compared to the low-uptake cells. These differences were observed in naïve T cells as well as *in vitro* activated T cells. It was also demonstrated that the high-uptake cells are more metabolically active than the low-uptake cells, in line with existing literature about effector T cell metabolism. The metabolic differences were also reflected

on a proteomic and transcriptomic level where key proteins and genes involved in glycolysis, fatty acid synthesis and the mevalonate pathway were significantly upregulated in the high-uptake cells. The upregulation of these pathways is closely connected to the metabolic reprogramming that occurs during effector T cell differentiation (described in Chapter 1) and further supported the observation that high StA-uptake T cells exhibited a more effector-like state. However, it could not be determined if the high-uptake cells are inherently dispositioned for a more effector-like state, or if this is induced by increased availability of FAs in the culture medium.

In conclusion, this thesis reports the first use of StA as a bioorthogonal analogue of OA. StA was readily taken up *in vitro* by a plethora of immune cells and could react with tetrazine-modified reporter molecules (e.g. fluorophores) via an IEDDA reaction, presenting a non-toxic, live-cell compatible alternative to other commonly used bioorthogonal reactions. The versatility of this approach allowed for multiplexing with other bioorthogonal reactions, permitting the simultaneous study of multiple biomolecules. The workflow could further be adapted and applied to study the lipidation of proteins as a PTM, as well as to investigate phenotypic and multiomic differences between T cells with a differential StA-uptake. The adaptability of the workflow emphasises its strength and applicability as a chemical tool to study FA uptake.

Future Prospects

Effects of different spacer lengths on pull-down of oleoylated proteins

In Chapter 3, a library of cell-permeable tetrazine-modified biotins were synthesised. Of these, compounds **17** and **19** were found to be cell-permeable and reactive with StA. However, the compounds had two different spacers between the biotin moiety and the tetrazine, with either a short (~13 Å, biotin) or medium (~22 Å, LC-biotin) spacer length (Figure 1A). These cell-permeable biotins were compared to the cell-impermeable biotin-PEG4-tetrazine which has a long (~29 Å) spacer between the biotin and tetrazine moieties (Figure 1A). In the chapter it was postulated that the short and medium spacer lengths of **17** and **19** could lead to increased steric hindrance upon binding of the tetrameric streptavidin beads during pull-down, leading to fewer proteins being detected. This effect was not observed for biotin-PEG4-tetrazine, further supporting the hypothesis that spacer length plays a role in protein retrieval.

In view of these findings, an expansion of the library of cell-permeable tetrazine-modified biotins is envisioned, where an additional spacer length similar to that of PEG4 is added (Figure 1B, LC-LC-biotin). However, increasing spacer length also appeared to negatively impact the compounds' solubility, so this would need to be optimised further. A cell-impermeable biotin-PEG2-tetrazine could also be used as a control, since it also has a medium spacer length (Figure 1B). If a drastic drop in detected proteins occurs compared to biotin-PEG4-tetrazine, spacer length is likely implicated, and a longer spacer would lead to less steric hindrance.

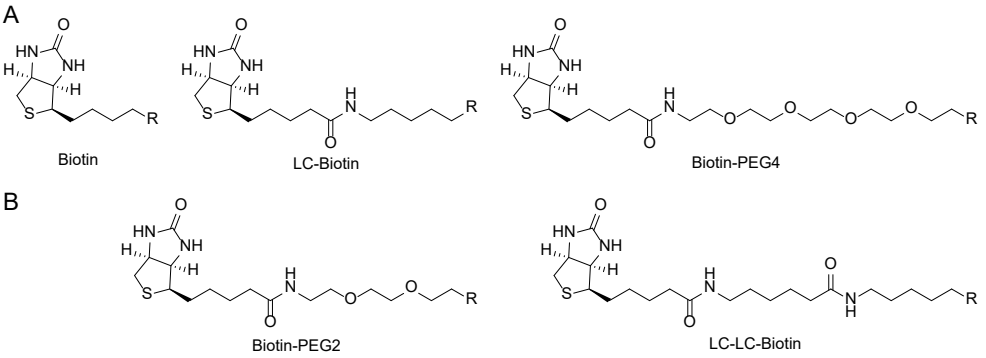

Figure 1: *Structures of biotin molecules with different spacer lengths.* ***A)*** *biotin, LC-biotin and biotin-PEG4,* ***B)*** *biotin-PEG2 and LC-LC-biotin.*

Incorporating fatty acid uptake into the single-cell RNAseq workflow

Chapter 4 described how information about fatty acid uptake was multiplexed with a single-cell RNA sequencing (scRNAseq) workflow by using StA. Cells were treated with StA, and subsequent IEDDA reaction with a fluorophore, before being sorted into high- and low-uptake populations by FACS. The two resulting populations were subjected to scRNAseq and were compared to each other. However, this strategy requires a sorting step during which information of nutrient uptake *per individual cell* is lost, preventing the correlation of sequencing information to nutrient uptake on a per-cell basis.

A different strategy was therefore also attempted, with the idea that the StA-uptake information could be incorporated directly as a readable parameter in the scRNAseq workflow. For this purpose, an oligonucleotide barcode system was developed that was inspired by the TotalSeq™ B barcoding technology. This technology was developed to be compatible with 10x Genomics' scRNAseq platform and consists of an antibody conjugated to the 5' end of an oligonucleotide (Figure 2A). The antibody is specific for a cell surface marker of interest, and the oligonucleotide firstly consists of a capture sequence which is implemented in the 10x Genomics workflow. In addition, a PCR handle is included for amplification, as well as the barcode sequence itself which is unique to each TotalSeq™ B antibody used.

The newly developed oligonucleotide described here consisted of a TotalSeq™ barcode conjugated to a methyltetrazine at the 5' end, rather than to an antibody (Figures 2B & 2C). This would allow for it to react in an inverse electron-demand Diels-Alder (IEDDA) click reaction to StA, thereby allowing the quantification of StA in the same sequencing run that would analyse the per-cell transcriptome.

The initial experiments with the tetrazine-conjugated oligonucleotide were performed with the murine dendritic cell line DC2.4, which had been prelabelled with StA, before being fixed and permeabilised. The perforation of the cell membrane allowed for the tetrazine-conjugated oligonucleotide to enter the cells to react with StA. As a negative control, cells prelabelled with native OA were used. After the IEDDA

reaction, unreacted oligonucleotide was washed away. The cells were then prepared according to 10x Genomics' provided instructions, and the PCR product was analysed on an Agilent Bioanalyzer chip. Unfortunately, no substantial difference in the amount of PCR product was observed between the StA- and OA-treated cells (Figure 2D). Some optimisation was attempted. For example, by increasing the cell numbers, or increasing the number of wash steps after the IEDDA click reaction. However, nothing appeared to affect the amount of PCR product detected in the StA sample compared to the OA sample (data not shown).

It was hypothesised that since FAs are not covalently crosslinked upon fixation with paraformaldehyde, and the water solubility of StA is massively increased upon click reaction with the oligonucleotide, the entire StA-oligonucleotide complex could potentially be washed away during the wash steps after the click reaction. It is also not known what effect the conjugation of the oligonucleotide to the tetrazine has on its reactivity with cyclopropenes, and it is possible that the kinetics of the tetrazine-conjugated oligonucleotide are so slow that one hour incubation for the click reaction was not sufficient. It was shown in Chapter 3 that the addition of bulky groups to the tetrazine can largely impact its ability to react with StA. Due to these major unanswered technological questions, as well as time- and cost-constraints, this approach was abandoned for the time being.

Although the initial tests with the tetrazine-conjugated oligonucleotide in combination with StA did not show positive results, it would be interesting to try this approach with other nutrients, e.g. amino acids, that are covalently crosslinked upon fixation. This would remove the uncertainty of washing away the nutrient after IEDDA reaction with the oligonucleotide and would better demonstrate the feasibility of the approach.

Effects of starvation prior to fatty acid uptake

To build further on the data described in Chapter 4, there are several new angles that could be interesting to explore. T cells undergo metabolic reprogramming upon activation, which renders effector T cells reliant on uptake of exogenous nutrients (see Chapter 1). Upon nutrient deficiency, for example by metabolic competition for glucose in the tumour microenvironment, effector T cell differentiation and function are negatively impacted.[9,10] Glucose deficiency could also skew T cell differentiation in favour of regulatory T cells over effector T cells.[11] While the StA uptake in Chapter 4 was performed in complete culture medium, it would be interesting to see how the T cells would react to starvation, e.g. by using glucose-depleted culture medium, prior to StA uptake, and if this would affect the observed effector-like state of the high-uptake T cells (see Chapter 4).

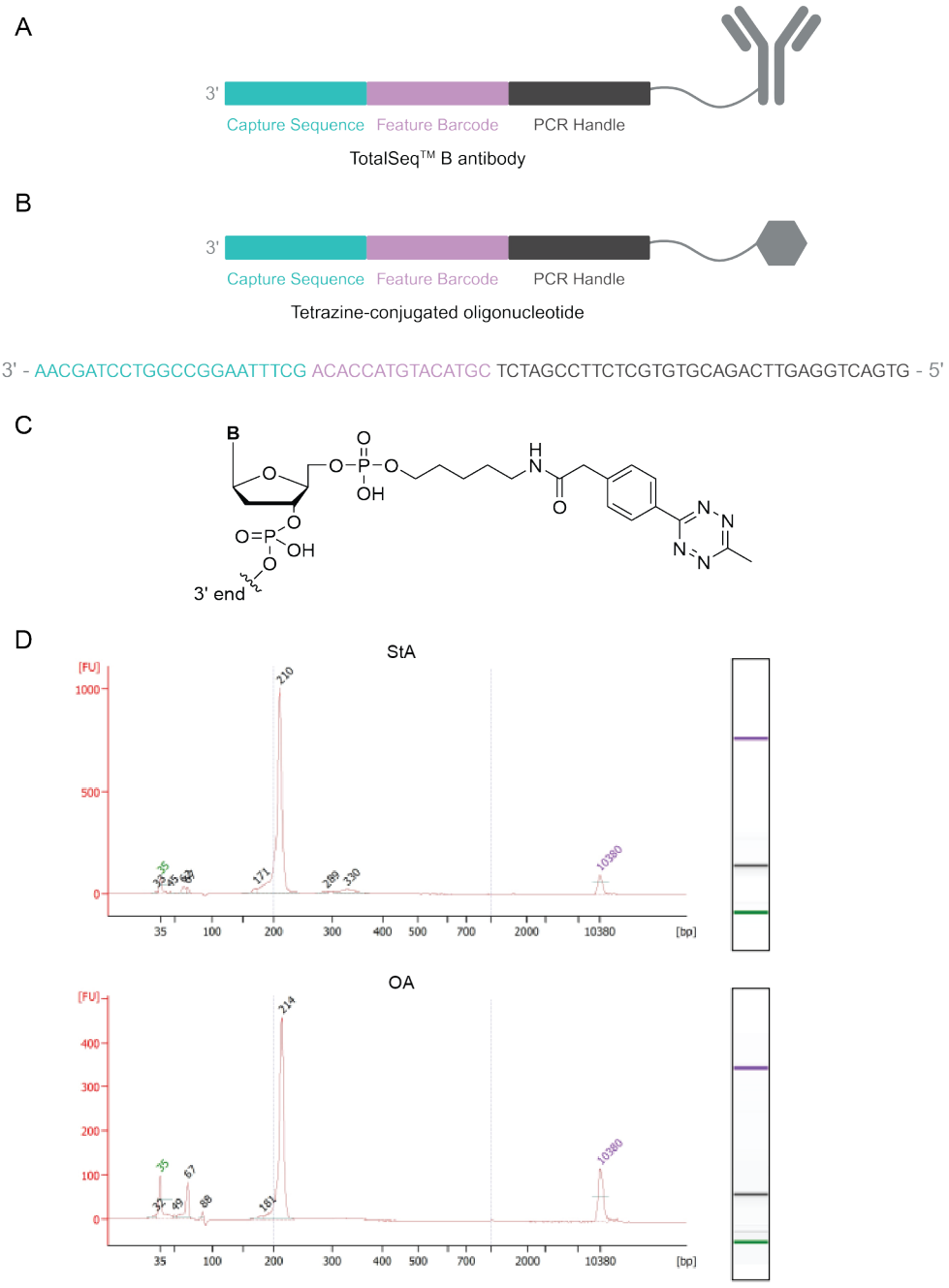

Figure 2: A) *TotalSeq™ B feature barcoding technology developed for antibody labelling of surface markers to be implemented into the 10x Genomics workflow.* ***B)*** *TotalSeq™ B-inspired oligonucleotide barcode with tetrazine modification at 5' end, and the oligonucleotide sequence.* ***C)*** *Structure of 5' tetrazine modification on the oligonucleotide.* ***D)*** *example of PCR results after StA uptake and IEDDA reaction with the tetrazine-modified oligonucleotide.*

Further classifications of T cell subsets upon differential FA uptake

It would also be interesting to further analyse and classify which T cell subsets are present in the high and low StA-uptake populations after FACS (see Chapter 4). The cytokine production of the two different populations could be analysed by enzyme-linked immunosorbent assays (ELISAs), or the populations could be subjected to further flow cytometry analysis with a more elaborate and thorough antibody panel. This could help determine the present T cell subsets in more detail and further verify if the high-uptake population contains a higher proportion of effector T cells.

To investigate the differentiation potential of the high and low StA-uptake populations of naïve splenocytes, the cells could be activated *in vitro* with αCD3/αCD28 antibodies after FACS. After the *in vitro* activation, a similar combination of ELISAs and flow cytometry as described above could be applied to determine which T cell subsets are predominantly present, and if there are differences between cells with differential FA uptake capacities.

Multiplexing nutrients in the single-cell RNAseq workflow

In Chapter 2 it was demonstrated that the IEDDA reaction with StA can be multiplexed with other bioorthogonal reactions and used to study multiple biomolecules at once. This could be extrapolated to the scRNAseq workflow described in Chapter 4, where a second bioorthogonal nutrient analogue, and subsequent bioorthogonal reaction, could be added. The bioorthogonal amino acid analogue azidohomoalanine, which has been shown to mimic glutamine uptake in T cells[12], could for example be used. However, a bioorthogonal reaction must be chosen that does not utilise a copper catalyst, since the copper catalyst was shown to degrade RNA (Chapter 4, Figure S2). For this purpose, a strain-promoted azide-alkyne cycloaddition (SPAAC)[13] or Staudinger ligation[14] could be used, although some further optimisations would be necessary to incorporate this into the scRNAseq workflow. Since T cells also increase their amino acid uptake upon differentiation into effector T cells (see Chapter 1), it is likely that cells with a high FA uptake will also show a high amino acid uptake. However, there could be populations of cells with a high FA uptake combined with a low amino acid uptake and vice versa. It would be interesting to determine which phenotypic, metabolic, and transcriptomic profile these cells have, and what differentiate them from the other T cell populations.

Acknowledgements

The Leiden Genome Technology Centre (LGTC) at Leiden University Medical Centre (LUMC) are acknowledged for their help with developing and testing of the oligonucleotide barcode approach.

Materials & Methods

General. Sterculic acid was purchased from Cayman Chemical (#26735), and stored as 10 mM or 100 mM stock solutions in DMSO at -20°C. Oleic acid was purchased from Sigma Aldrich (#O1383), and stored as 100 mM stock solution in DMSO at -80°C. The murine RNase inhibitor was purchased from New England Biolabs (#M0314L), and stored as delivered at -20°C. The RNase-free PBS (10x) was purchased from Thermo Fisher Scientific (#J62851.AP**)** and stored as delivered at room temperature (RT). The PBS was diluted to 1x with MilliQ water prior to use. The custom-made oligonucleotide sequence with a 5' tetrazine modification (Figures 2B & 2C) was ordered from Biomers.net. Upon delivery, the oligonucleotide was dissolved in MilliQ water (1 mM), and stored at -20°C.

DC2.4 cell culturing. DC2.4 cells were cultured in RPMI 1640 culture medium (Gibco, #31870025) supplemented with 10% FCS, GlutaMAX (2 mM), sodium pyruvate (1 mM), 1x non-essential amino acids (NEAA, Thermo Fisher Scientific), penicillin (100 I.U./mL), streptomycin (50 µg/mL), and 2-mercaptoethanol (50 µM, Thermo Fisher Scientific), and incubated at 37°C, 5% CO_2. The cells were grown to 70-80% confluency and passaged every 2-3 days by trypsinisation.

Click reaction with ssDNA barcode modified with tetrazine. $2.5x10^6$ DC2.4 cells were seeded per 60 mm dish, and incubated at 37°C, 5% CO_2 overnight to allow the cells to attach. The samples were treated with either sterculic acid or the native oleic acid (50 µM) in fresh DC2.4 medium, and incubated for 1 h at 37°C, 5% CO_2, to allow for uptake of the FAs. The cells were washed with fresh medium x1, followed by PBS x1, before they were scraped in PBS and transferred to Eppendorf tubes. The cells were spun down at 400 rcf for 5 min, and were fixed in 4% PFA in PBS for 15 min at RT. The cells were spun down at 400 rcf for 5 min, before unreacted PFA was quenched with PBS supplemented with glycine (20 mM) and RNase inhibitor (40 U/mL). The cells were spun down at 900 rcf for 5 min, and washed with RNase-free PBS x1 before permeabilisation with RNase-free PBS supplemented with saponin (0.1%) for 15 min at RT. The tubes were filled up with RNase-free PBS before being spun down at 850 rcf for 5 min. The custom-made tetrazine-conjugated oligonucleotide (5 µM, see Figures 2B & 2C) in RNase-free PBS, supplemented with RNase inhibitor (40 U/mL), was added to the cells and reacted for 1 h at RT with shaking (800 rpm). The cells were spun down at 850 rcf for 5 min and was washed with RNase-free PBS between 2 and 5 times. The cells were resuspended in RNase-free PBS and was transported on ice to collaborators from the Leiden Genome Technology Center (LGTC) at Leiden University Medical Center (LUMC). The samples were thereafter prepared according to the 10x Genomics user guide (CG000477), until having been analysed on an Agilent Bioanalyser (see results in Figure 2D).

References

1. O'Neill, L. A. J., Kishton, R. J. & Rathmell, J. A guide to immunometabolism for immunologists. *Nat Rev Immunol* **16**, 553–565 (2016).
2. Buck, M. D., O'Sullivan, D. & Pearce, E. L. T cell metabolism drives immunity. *Journal of Experimental Medicine* **212**, 1345–1360 (2015).
3. MacIver, N. J., Michalek, R. D. & Rathmell, J. C. Metabolic Regulation of T Lymphocytes. *Annu Rev Immunol* **31**, 259–293 (2013).
4. Jacobs, S. R. *et al.* Glucose Uptake Is Limiting in T Cell Activation and Requires CD28-Mediated Akt-Dependent and Independent Pathways. *The Journal of Immunology* **180**, 4476–4486 (2008).
5. Geiger, R. *et al.* L-Arginine Modulates T Cell Metabolism and Enhances Survival and Anti-Tumor Activity. *Cell* **167**, 829–842 (2016).
6. Sinclair, L. V *et al.* Control of amino-acid transport by antigen receptors coordinates the metabolic reprogramming essential for T cell differentiation. *Nat Immunol* **14**, 500–508 (2013).
7. Carr, E. L. *et al.* Glutamine Uptake and Metabolism Are Coordinately Regulated by ERK/MAPK during T Lymphocyte Activation. *The Journal of Immunology* **185**, 1037–1044 (2010).
8. Angela, M. *et al.* Fatty acid metabolic reprogramming via mTOR-mediated inductions of PPARγ directs early activation of T cells. *Nat Commun* **7**, (2016).
9. Chang, C.-H. *et al.* Metabolic Competition in the Tumor Microenvironment Is a Driver of Cancer Progression. *Cell* **162**, 1229–1241 (2015).
10. Ho, P.-C. *et al.* Phosphoenolpyruvate Is a Metabolic Checkpoint of Anti-tumor T Cell Responses. *Cell* **162**, 1217–1228 (2015).
11. Feuerer, M. *et al.* Lean, but not obese, fat is enriched for a unique population of regulatory T cells that affect metabolic parameters. *Nature Medicine* **15**, 930–939 (2009).
12. Pelgrom, L. R. *et al.* QUAS-R: An SLC1A5-mediated glutamine uptake assay with single-cell resolution reveals metabolic heterogeneity with immune populations. *Cell Rep* **42**, (2023).
13. Agard, N. J., Prescher, J. A. & Bertozzi, C. R. A Strain-Promoted [3 + 2] Azide−Alkyne Cycloaddition for Covalent Modification of Biomolecules in Living Systems. *Journal of the American Chemical Society* **126**, 15046–15047 (2004).
14. Kiick, K. L., Saxon, E., Tirrell, D. A. & Bertozzi, C. R. Incorporation of azides into recombinant proteins for chemoselective modification by the Staudinger ligation. *Proceedings of the National Academy of Sciences* **99**, 19–24 (2002).